

STELLAR MODEL CHROMOSPHERES. IV. THE FORMATION OF THE $H\epsilon$ FEATURE IN THE SUN (G2 V) AND ARCTURUS (K2 III)

THOMAS R. AYRES AND JEFFREY L. LINSKY*

Joint Institute for Laboratory Astrophysics, University of Colorado and
 National Bureau of Standards, Boulder

Received 1975 February 17

ABSTRACT

The formation of the Balmer series member $H\epsilon$ in the near red wing of the Ca II H line is discussed for two cases: the Sun ($H\epsilon$ absorption profile) and Arcturus ($H\epsilon$ emission profile). It is shown that although the $H\epsilon$ source functions in both stars are dominated by the Balmer continuum radiation field through photoionizations, the line formation problems in the two stars are quantitatively different, owing to a substantial difference in the relative importance of the stellar chromosphere temperature inversion compared with the stellar photosphere.

Subject headings: chromosphere, solar — chromosphere, stellar — line profiles — radiative transfer — stars, individual

I. INTRODUCTION

In the previous paper of this series (Ayres and Linsky 1975, hereafter Paper III) we proposed a model upper photosphere and chromosphere for the K giant Arcturus (K2 III) consistent with the measured emission in the resonance lines of Ca II (H and K) and Mg II (*k* only), assuming complete redistribution, and the flux profiles of the H and K damping wings in a coherent scattering approximation. In this paper we continue our discussion of the outer atmospheres of late-type stars by applying our inferred model for Arcturus and current solar models (Vernazza *et al.* 1973, 1975; Ayres *et al.* 1975) to an investigation of the curious behavior of the hydrogen Balmer line $H\epsilon$, which is commonly seen in emission in late-type stars, especially K and M giants (Wilson 1957), but not in the Sun. The other members of the Balmer series are invariably pure absorption lines in those stars showing $H\epsilon$ in emission (Wilson 1957) and the $H\epsilon$ feature is formed only 1.6 Å redward of the strong Ca II λ 3969 H line core. On this basis previous studies of the $H\epsilon$ formation problem (Ayres and Linsky 1974; Fosbury 1974) have drawn an analogy between stellar $H\epsilon$ emission and the rare-earth emission lines seen against the background of the solar limb H and K damping wings (Canfield 1971*a, b*) and also in Arcturus (Fosbury 1971). For both classes of spectral features a "suprathermal" source function is responsible for the observed emission relative to the thermal background provided by the H (or K) line wing, although the particular mechanisms that control the line source functions in each case are quite different (radiative interlocking for the rare earths; photoionization domination for the Balmer line). Unfortunately, both of the previous discussions of the $H\epsilon$ formation problem are largely qualitative, and neither is based

on an examination of the radiative transfer problem comparable in detail, for instance, to Canfield's study of the solar rare-earths emission. We hope to remedy this situation by presenting a series of illustrative solutions of the $H\epsilon$ transfer problem for realistic model atmospheres of two stars: the Sun, which shows $H\epsilon$ in absorption relative to the H line wing; and Arcturus, which is the archetypical case for $H\epsilon$ "emission" (Wilson 1938, 1957; Wellmann 1940; Popper 1956).

Although our illustrative calculations for the most part substantiate the previous work of Ayres and Linsky (1974) and Fosbury (1974), we find several significant differences, in particular the role played by the chromospheric temperature inversion in cool stars.

The paper is divided into sections as follows: in § II we present the observed profiles of $H\epsilon$ for the Sun and Arcturus; § III is devoted to the formulation of the radiative transfer problem, the ionization equilibrium solution, and a description of the model atmospheres adopted for the illustrative calculations; in § IV we discuss the radiative and collisional rate coefficients for the model hydrogen atom; in § V we solve the line formation problem for the range of models and rates proposed in the previous sections; and finally, in § VI we comment on the significance of our illustrative calculations in light of the observed behavior of the $H\epsilon$ feature in late-type stars (e.g., Wilson 1957).

II. OBSERVATIONS

Stars such as the Sun and Arcturus show $H\epsilon$ as a relatively weak feature against the sloping background of the Ca II H line wing. Because the H wing in the vicinity of $H\epsilon$ is itself only 10-20 percent the intensity of the neighboring "continuum," spectra of this interval with adequate detail for the profile synthesis approach require high dispersion, good photon statistics, and low scattered light. $H\epsilon$ spectra of suitable quality are

* Staff member, Laboratory Astrophysics Division, National Bureau of Standards.

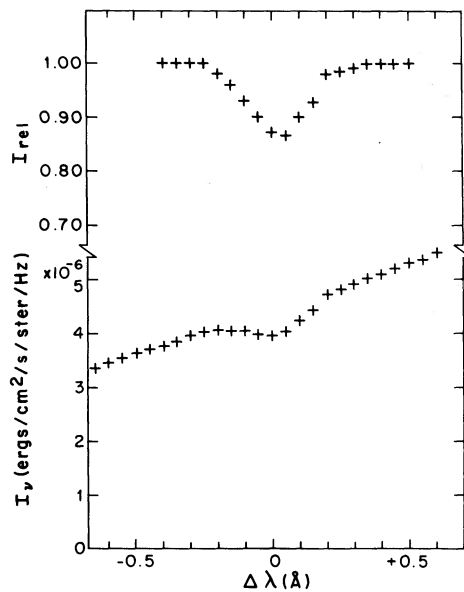


FIG. 1.—Absolute and relative intensity profiles for the solar $H\epsilon$ absorption feature. A multi-line blend in the red wing of $H\epsilon$ has been omitted.

routinely available for the Sun, but are more difficult to obtain for Arcturus.

a) The Solar Absorption Profile

As with most F through early K dwarfs, the Sun shows $H\epsilon$ in absorption relative to the H line wing. The solar profile of $H\epsilon$ we consider here is based on the double-pass measurements of the quiet-Sun H wing by Shine (1973) as calibrated by Houtgast's (1970) absolute photometry. From the observed profile we

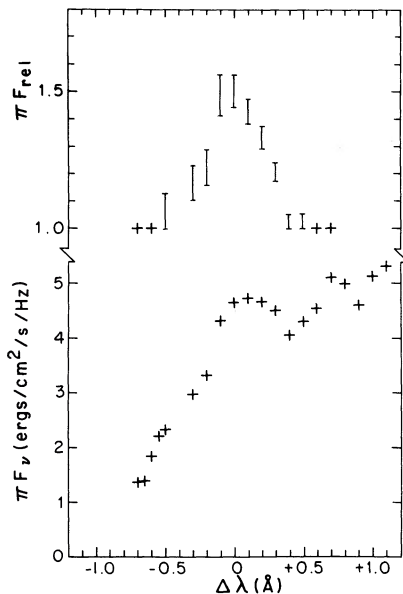


FIG. 2.—Absolute and relative flux profiles for the Arcturus $H\epsilon$ emission feature. Unit flux equals 10^{-7} cgs.

construct a “relative intensity” profile by taking the ratio of the measured intensities against an interpolated H wing background. This latter representation of the $H\epsilon$ profile is useful in comparisons with synthesized spectra. Both profiles are illustrated in Figure 1.

b) The Arcturus Emission Feature

$H\epsilon$ emission was first noted in Arcturus by Wilson (1938), and subsequently by Wellmann (1940) and Popper (1956). We adopt the $H\epsilon$ flux profile from Griffin's (1968) *Photometric Atlas* as calibrated by Willstrop's (1965, 1972) absolute photometry (see Paper III). The Arcturus $H\epsilon$ feature and the corresponding relative flux profile are illustrated in Figure 2. The error bars on the latter data refer to the slight ambiguity in interpolating the H wing across the $H\epsilon$ profile. Note that the solar $H\epsilon$ absorption is relatively weak (10–15% maximum contrast) compared with the Arcturus $H\epsilon$ emission (40–50% maximum contrast).

III. FORMULATION OF THE TRANSFER PROBLEM; THE IONIZATION EQUILIBRIUM; AND THE ADOPTED MODEL ATMOSPHERES

The transfer problem for the optically thick hydrogen lines is complicated by the fact that atomic hydrogen is the dominant constituent of normal stellar atmospheres. The complication arises from the dependence of the ionization equilibrium of the atmosphere at each depth on the statistical equilibrium of the hydrogen atoms. This is in general a nonlinear problem because the statistical equilibrium of hydrogen is controlled by a complex interplay of radiative and collisional rates, which in turn are determined by characteristics of the atmosphere. Hence, the structure of the atmosphere and the line formation problem in hydrogen are strongly coupled through the ionization equilibrium.

a) The Line Formation Problem

We use the complete linearization method of Auer and Mihalas (1969) as embodied in the Auer *et al.* (1972) code LINEAR to solve the non-LTE line formation problem for $H\epsilon$. In order to include all of the important routes into and out of the upper and lower levels of the $H\epsilon$ transition ($n = 7$ and $n = 2$, respectively), we consider a representation for hydrogen consisting of eight bound levels and the continuum. We allow for explicit transfer in the Lyman continuum and the Balmer lines $H\alpha$ through $H\zeta$, while assuming radiative detailed balance for the Lyman series. The latter approximation should be accurate in the low chromosphere and upper photosphere where the $H\epsilon$ contribution function peaks. All the remaining radiative transitions are assumed to be optically thin.

In addition to the usual continuous opacity sources (see Auer *et al.* 1972) we include the Ca II H line wing as a frequency-independent background opacity for the $H\epsilon$ transition. Fortunately, $H\epsilon$ is formed far enough beyond the Doppler core of the H line that the Ca II

populations are not influenced by the presence of the Balmer line (see also Lites 1974). We specify the emissivity at H ϵ due to the H line wing by solving a simple coherent scattering problem in the Eddington approximation (Mihalas 1970). This approach differs from the usual assumption of complete redistribution, in which case the wing source function would be thermalized to the local Planck function, but is probably more physical. In the coherent scattering approximation the H wing source function departs from the local Planck function at a given depth m by a factor $\beta(m)$:

$$S_\nu(m) \approx \beta(m)B_\nu[T_e(m)], \quad (1)$$

where

$$\beta(m) \approx \left\{ 1 - \frac{1 - \lambda_\nu}{1 + \lambda_\nu^{1/2}} \left(1 - \frac{2 + \sqrt{3}}{3\tau_\nu} \frac{d \ln B_\nu}{d \ln \tau_\nu} \right) \times \exp [-(3\lambda_\nu)^{1/2}\tau_\nu] \right\}. \quad (2)$$

Here $\tau_\nu = \tau_\nu(m)$ is the monochromatic optical depth in the H wing at $\lambda = \lambda_{H\epsilon}^{(0)}$, and λ_ν is the incoherence fraction

$$\lambda_\nu = \frac{a + \Gamma}{1 + a}. \quad (3)$$

The first term in the numerator of the incoherence fraction accounts for the radiative mixing provided by the subordinate infrared triplet line $\lambda 8662$, $a \sim 0.058$ independent of density, while the second term

$$\Gamma \approx \frac{1.08(n_H/10^{16})}{1.0 + 1.08(n_H/10^{16})} \quad (4)$$

is the normalized ratio of pressure broadening to radiative damping. We have ignored additional terms representing inelastic collisions because they are small compared with a or Γ .

We assume that the background contributions to the total emissivity at H ϵ due to "continuum" sources other than the H line wing are in LTE. Hence the total background opacity at H ϵ is

$$\kappa_\nu^{\text{background}} = \kappa_\nu^c + \kappa_\nu^{\text{H wing}} \quad (5)$$

and the corresponding emissivity is

$$\eta_\nu^{\text{background}} = (\kappa_\nu^c + \kappa_\nu^{\text{H wing}}\beta)B_\nu(T_e). \quad (6)$$

We approximate the line absorption coefficients for the six Balmer lines treated explicitly with depth-dependent Doppler profiles, and assume complete redistribution in the formulation of the transfer problem. For simplicity we ignore turbulent broadening in the Doppler width, because in practice thermal broadening of hydrogen will dominate over any subsonic motions. Finally, we solve the Lyman continuum problem in eight equally spaced frequency bands from the ionization edge at $\nu_0 = 3.29 \times 10^{15}$ Hz to $\nu = 4.0 \times 10^{15}$ Hz. All but a negligible fraction of the total Lyman continuum (LyC) emission of both the

Sun and Arcturus is contained within this frequency interval.

b) The Ionization Equilibrium

The atmospheric models we consider here are plane-parallel, homogeneous, and hydrostatic. The justifications for—and objections to—this approach are discussed in detail elsewhere (e.g., Paper III; Linsky and Avrett 1970; Vernazza *et al.* 1973). We specify a model by the run of kinetic temperature T_e (K) with mass column density m (g cm $^{-2}$). The choice of "mass" as an independent depth variable is motivated partly by the irrelevance of the conventional "height" scale for stellar work, but mostly because the hydrostatic equilibrium condition has a particularly simple form in the "mass" representation, especially when radiation pressure can be neglected. At each depth the pressure is $P_{\text{gas}} = gm$, where g is the surface gravity. Assuming that the stellar plasma is a perfect gas gives the total number density at each pressure

$$n_{\text{tot}} = P_{\text{gas}}/kT_e = \left(1 + A_{\text{He}} + \sum_{\xi} A_{\xi} \right) n_{\text{H}} + n_e. \quad (7)$$

Here A_{He} is the abundance of helium relative to hydrogen, the A_{ξ} are abundances of elements heavier than helium, $n_{\text{H}} = n_{\text{H I}} + n_p$, $n_{\text{H I}}$ is the neutral hydrogen density, n_p is the proton density, and n_e is the electron density. We have neglected the formation of molecular hydrogen which is not a particularly important sink for atomic hydrogen even at the low temperatures of a K giant atmosphere. The individual number densities are further related by charge conservation,

$$n_e = n_p + \left[\sum_{\xi} A_{\xi} \phi_{\xi}(T_e, n_e) \right] n_{\text{H}}, \quad (8)$$

and by the ionization balance for hydrogen,

$$n_{\text{H I}} = n_e n_p b_1 \psi_{\text{H}}(T_e) \cdot \tilde{U}_1 = \sum_{i=1}^N n_i. \quad (9)$$

Here, ϕ_{ξ} is the fractional degree of ionization of the ξ th metal (see Vernazza *et al.* 1973), ψ_{H} is the Saha factor for hydrogen, and \tilde{U}_1 is the inverse ratio of the fractional population of the ground state of hydrogen relative to the total neutral hydrogen population:

$$\tilde{U}_1 \equiv \left[n_1 / \sum_{i=1}^N n_i \right]^{-1} = \left(1 + \sum_{n=2}^N \frac{b_n}{b_1} \tilde{\psi}_n \right). \quad (10)$$

In the above the b_n are departure coefficients;

$$\tilde{\psi}_n = n^2 \exp [-\chi_{\text{H}}(1 - 1/n^2)/kT_e], \text{ with } \chi_{\text{H}} = 13.6 \text{ eV}, \quad (11)$$

and N refers to the last distinct energy level below the ionization limit (which is depressed owing to the effect of the finite electron pressure).

Given the run of temperature with mass column density, the atomic abundances, and the departure

coefficients b_n , we can uniquely derive all of the relevant number densities, in particular the electron density. Again, this problem is inherently nonlinear because the departure coefficients are themselves determined by the model atmosphere. We adopt the standard approach for solving the coupled statistical equilibrium of the model atom and the ionization equilibrium of the model atmosphere of iterating back and forth between the radiative transfer solution and the number density calculation. We find that adequate self-consistency in the electron density can be achieved using a simplified model hydrogen atom consisting of three levels and the continuum, allowing for transfer in the LyC and H α . This approach is similar to that used by Noyes and Kalkofen (1970) in their analysis of the solar chromosphere.

c) The Adopted Model Atmospheres

For the sake of numerical tractability we consider only a limited range of model atmospheres for the Sun and Arcturus. We adopt as our principal solar model the temperature distribution of Vernazza *et al.* (1973; 1975 hereafter V-A-L) which was constructed to fit a broad range of calibrated solar continuum data, from the extreme-ultraviolet to the far-infrared. The photospheric portion of the V-A-L model is similar to the Gingerich *et al.* (1971) HSRA (except for $\tau_{5000} > 1$), however, the chromospheric temperature structure differs substantially. In particular the V-A-L model has a broad temperature plateau in the low chromosphere at $T_e \approx 6000$ K following a steep rise from the adopted temperature minimum of 4150 K. For illustrative purposes we also consider an alternative set of solar models based on an upper photospheric temperature distribution inferred from the Ca II H and K line wings using a coherent scattering approximation (Ayles *et al.* 1975). These models differ from the V-A-L model primarily in the surface layers of the upper photosphere above $\tau_{5000} \approx 10^{-2}$. In fact the inferred temperature minimum consistent with the intensities of the observed K₁ minimum features is almost 300 K hotter than the V-A-L value of T_{\min} (see also Shine *et al.* 1975). In addition, for the alternative solar models we adopt schematic chromospheric temperature rises which are linear in $\log m$ up to $\tau_{\text{LyC}} = 1$. The latter is chosen to occur at $T_0 = 8000$ K. The motivation for this particular choice of an "upper boundary condition" is discussed in Paper III. We consider a pair of such models with values of $m_0 = 10^{-5.0}$ (model A) and $10^{-5.5}$ (model B) where $m_0 \equiv m(\tau_{\text{LyC}} = 1)$. The equivalent "top pressures" $P_0 = gm_0$ of these models bracket the observed pressure of the quiet-Sun upper chromosphere and transition region, $P_0 = 0.15$ dyn cm^{-2} as inferred from extreme-ultraviolet emission lines (Dupree 1972). Above $T_0 = 8000$ K the temperature rises exponentially to $T_e = 10,000$ K to mimic the onset of a steep transition region temperature gradient.

The three solar models are illustrated in Figure 3.

In Paper III, we constructed a grid of model chromospheres for Arcturus consistent with the ob-

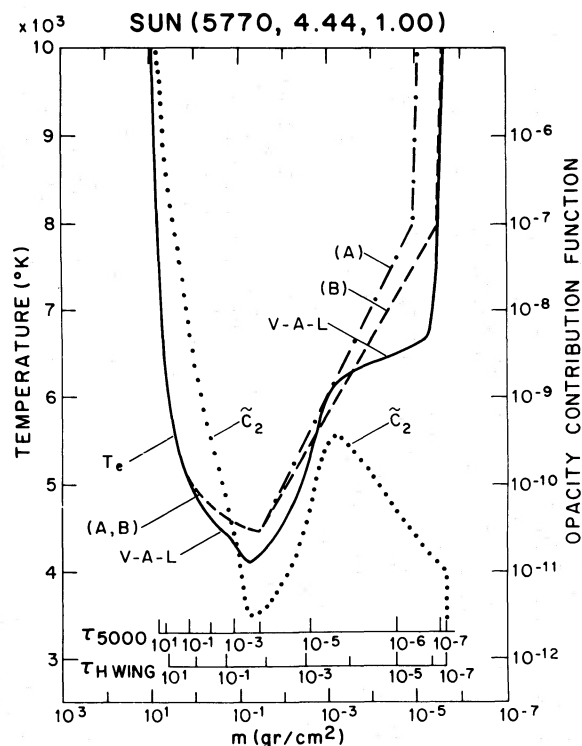


FIG. 3.—Adopted solar atmosphere models. The notation $\tau_{\text{H wing}}$ is the optical depth scale in the H line wing at the wavelength of H ϵ ; \tilde{c}_2 is the opacity contribution function defined by equation (20).

served range of Ca II H and K and Mg II k emission in the complete redistribution approximation, and an upper photosphere temperature distribution consistent with the damping wing profiles of H and K. As in Paper III, we assume $T_{\text{eff}} = 4250$ K, $g = 50$ cm s^{-1} , and metal abundances 30 percent of solar normal. Using linear temperature rises as described above for the alternative solar models, and the same value of $T_0 = 8000$ K, we found that the range of "top masses" $m_0 = 10^{-4.5}$ to $10^{-5.0}$ is consistent with the observed Ca II and Mg II emission of Arcturus. For our calculations here we will use three of these models covering a decade in m_0 , $m_0 = 10^{-4.5}$ ("C"), $10^{-5.0}$ ("D"), and $10^{-5.5}$ ("E"). The adopted chromosphere and upper photosphere temperature distributions are plotted in Figure 4. Note that the Arcturus temperature minimum of $T_{\min} = 3200$ K occurs much deeper in "mass" than its solar counterpart.

IV. RADIATIVE AND COLLISIONAL RATES

The radiative and collisional excitation and ionization rates play a central role in any line formation problem; hence an accurate knowledge of the rate coefficients is of fundamental importance. For the optically thick line and continuum transitions the radiative rates are determined in the course of the transfer solution. However, all of the collisional rates and the "background" radiative rates, i.e., those not

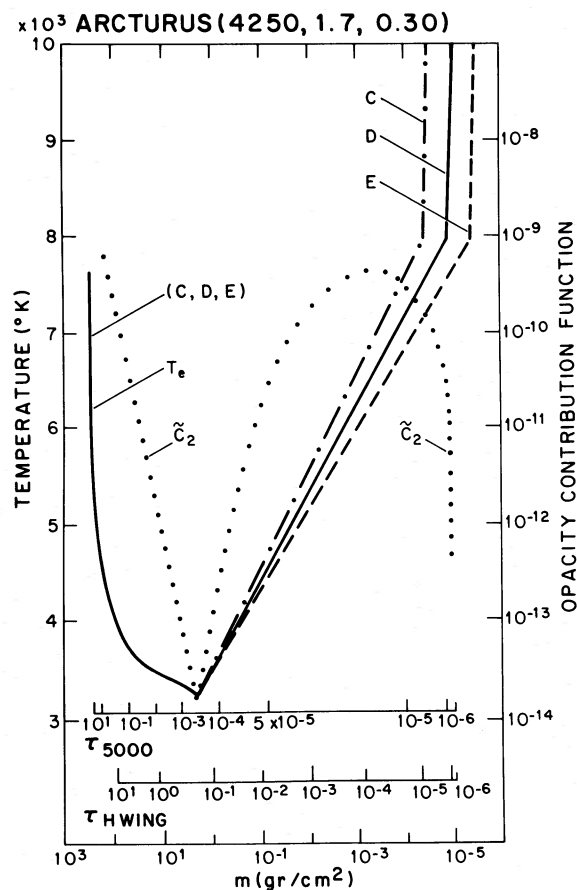


FIG. 4.—Adopted Arcturus atmosphere models

affected by the transfer solution, must of course be specified at the outset of the calculation. The radiative rates for the optically thin transitions can either be calculated explicitly from the model atmosphere using assumptions as to the background absorptivities and emissivities, in particular the line blanketing distribution functions, or these rates can be estimated from the emergent spectral energy distribution of the star. The photoabsorption cross sections come from experiment and theory, and are known exactly for hydrogen (e.g., Mihalas 1970). The collisional rates are products of temperature-dependent coefficients and the electron density. Unfortunately many of the hydrogenic collisional cross sections, especially those for bound-bound excitations with $l \geq 3$, have not been measured experimentally. For these coefficients we must turn to rough semiempirical estimates.

a) Collisional Rate Coefficients

We write the upward collision rate from levels l to u as

$$\Omega_{lu} = C_{lu}(T_e)n_e. \quad (12)$$

By detailed balancing the corresponding downward rate is

$$\Omega_{ul} = (n_l^*/n_u^*)\Omega_{lu}. \quad (13)$$

Here the n^* 's are LTE populations and $n_u^* = n_p$ when u is the continuum. For ionizations, we adopt the rate coefficients suggested by Mihalas (1967). These coefficients are based on the experimental cross sections of Kieffer and Dunn (1966; $l = 1$) and the theoretical results of Percival (1966; $l > 1$).

For $u = l + 1$ excitations we adopt the approximate rate coefficients of Golden and Sampson (1971), except for the resonance excitation $1 \rightarrow 2$ which is taken from the experimental results of Crandall *et al.* (1974). All remaining excitation rates $u > l + 1$ are based on the semiempirical estimates of Sampson and Golden (1970). In addition we have accounted for excitation to levels $u > 8$ by including the appropriate $l \rightarrow u$ rates in the l th collisional ionization coefficient. This approximation is equivalent to treating the upper levels in LTE. In practice, the required modification has little effect for $l \leq 5$; however, the increase in Ω_{lk} can be quite substantial for $l = 7$ and 8, and tends to force these levels closer to LTE.

b) Fixed Radiative Rates

We consider here the photoexcitation and photoionization rates for the optically thin hydrogen lines and continua. These rates are fixed during the radiative transfer calculation because they are intrinsic to the stellar spectral energy distribution and are not affected by changes in the hydrogen level populations as long as the relevant transitions are optically thin. Because we are principally concerned with the stellar upper photosphere and low chromosphere, all the hydrogen transitions are transparent in both the Sun and Arcturus with the obvious exceptions of the Lyman continuum, the Lyman lines, and the Balmer lines. For a photoionization the upward rate is given by

$$R_{lk} = \int_{-\infty}^{\infty} \frac{4\pi}{h\nu} \alpha_\nu J_\nu d\nu, \quad (14)$$

where

$$\begin{aligned} \alpha_\nu &= 0, & \nu < \nu_0 \\ &= \alpha_0(l)\nu^{-3}, & \nu \geq \nu_0 \end{aligned}$$

for hydrogen (Mihalas 1967), J_ν is the monochromatic mean intensity, and $\nu_0 = 3.29 \times 10^{15}/l^2$ Hz is the frequency at the l th bound-free absorption edge of hydrogen. The cross section $\alpha_0(l)$ has an additional weak frequency dependence due to the bound-free Gaunt factor.

Following the convention used by Auer *et al.* (1972) we rewrite the photoionization rate in terms of a radiation temperature

$$R_{lk} = \int_{\nu_0}^{\infty} \frac{4\pi}{h\nu} \alpha_\nu B_\nu(T_R) d\nu = \frac{8\pi}{c^2} \alpha_0(l) \nu_0^2 F\left(\frac{h\nu_0}{kT_R}\right). \quad (15)$$

Here,

$$F(x) = \sum_{n=1}^{\infty} E_1(nx),$$

where E_1 is the first exponential integral. In this formulation, the downward rate is simply

$$R_{kl} = \frac{8\pi}{c^2} \alpha_0(l) \nu_0^3 F \left(\frac{h\nu_0}{kT_e} \right) n_l^* / n_{\kappa}^*, \quad (16)$$

where n_l^* is the LTE population of level l and $n_{\kappa}^* = n_p$.

The excitation rate for bound-bound transitions has the same form as equation (14), except now $\alpha_v = \alpha_{lu} \phi_v$ is sharply peaked in frequency. In fact, since the radiation field is roughly constant over the narrow Doppler core of the line profile, we can approximate the photoexcitation rate as

$$R_{lu} = \frac{4\pi}{h\nu} \alpha_{lu} J_\nu; \quad \alpha_{lu} = \frac{\pi e^2}{mc} f_{lu}, \quad (17)$$

where f_{lu} is the oscillator strength of the transition. Again we rewrite the formal expression in terms of a radiation temperature

$$R_{lu} = \frac{4\pi}{h\nu} \alpha_{lu} B_\nu(T_R). \quad (18)$$

The corresponding downward rate is

$$R_{ul} = R_{lu} \frac{n_l^*}{n_u^*} \Big|_{T_e=T_R}. \quad (19)$$

At large optical depths, $J_\nu \rightarrow B_\nu$, hence $T_R \rightarrow T_e$; but near the "top" of the atmosphere ($\tau_\nu \ll 1$) the mean intensity falls to its surface value $J_\nu \rightarrow J_\nu^{(0)}$, hence $T_R \rightarrow T_R^{(0)}$. We approximate the true depth dependence of J_ν by setting $T_R = T_e$ for all depths below a reference level in the photosphere and $T_R = T_R^{(0)}$ above. The reference level corresponds to the monochromatic optical depth at which J_ν begins to thermalize to B_ν , but in general is not the depth where $T_e = T_R^{(0)}$.

We computed the necessary bound-bound and bound-free radiation temperatures on the basis of the observed spectral energy distributions of the Sun and Arcturus. For the Sun, calibrated observations covering virtually the entire spectrum are readily available (Thekaekara 1974; Vernazza *et al.* 1975), but for Arcturus we supplemented the narrow band photometry of Willstrop (1965) and the OAO-2 results of Doherty (1972) with fluxes synthesized using the semi-empirical model photosphere of § III. These synthesized fluxes have been crudely corrected for line blanketing using the blocking factors tabulated by Carbon and Gingerich (1969) for a model of similar effective temperature and gravity. From the spectral energy distribution $\pi F_\nu(0)$ we constructed the mean intensity distribution $J_\nu(0)$ using scaling factors C_ν , $C_\nu \equiv J_\nu(0)/\pi F_\nu(0)$, based on theoretical monochromatic limb darkening curves (Gingerich *et al.* 1971 for the Sun; Carbon and Gingerich 1969 for Arcturus). Finally, we numerically integrated the $J_\nu(0)$ distribution against the frequency-dependent photoionization

TABLE 1
FIXED PHOTOEXCITATION AND IONIZATION RATES

$l \rightarrow u$	$T_{\text{Rad}}(\text{K})$	
	Sun	Arcturus
2- κ	5060	3335
3- κ	4770	3395
4- κ	4500	3465
5- κ	4330	3595
6- κ	4200	3390
7- κ	3925	3175
8- κ	3705	2910
3-4.....	4140	3650
3-5.....	4560	3400
3-6.....	4550	3385
3-7.....	4640	3405
3-8.....	4670	3425
4-5.....	3520	2780
4-6.....	4000	3190
4-7.....	3980	3430
4-8.....	4040	3590
5-6.....	2800	2360
5-7.....	3290	2670
5-8.....	3480	2850
6-7.....	2490	2130
6-8.....	2820	2355
7-8.....	2300	2010

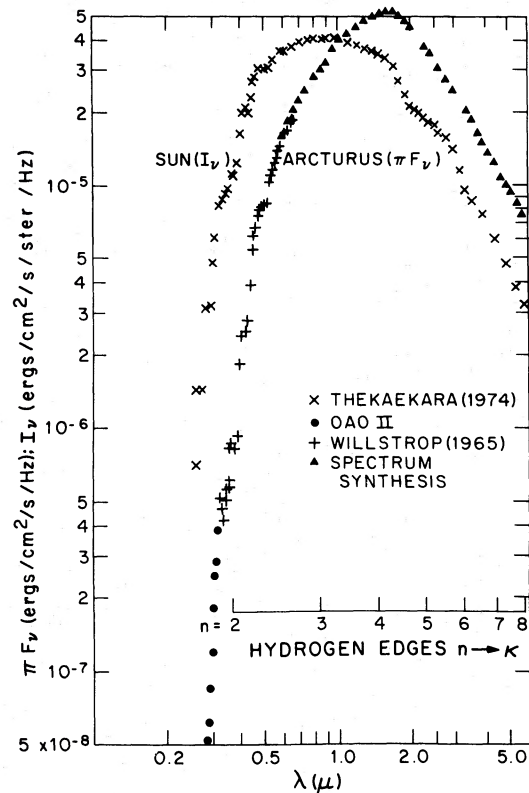


FIG. 5.—Absolute spectral energy distributions of the Sun (I_ν) and Arcturus (πF_ν).

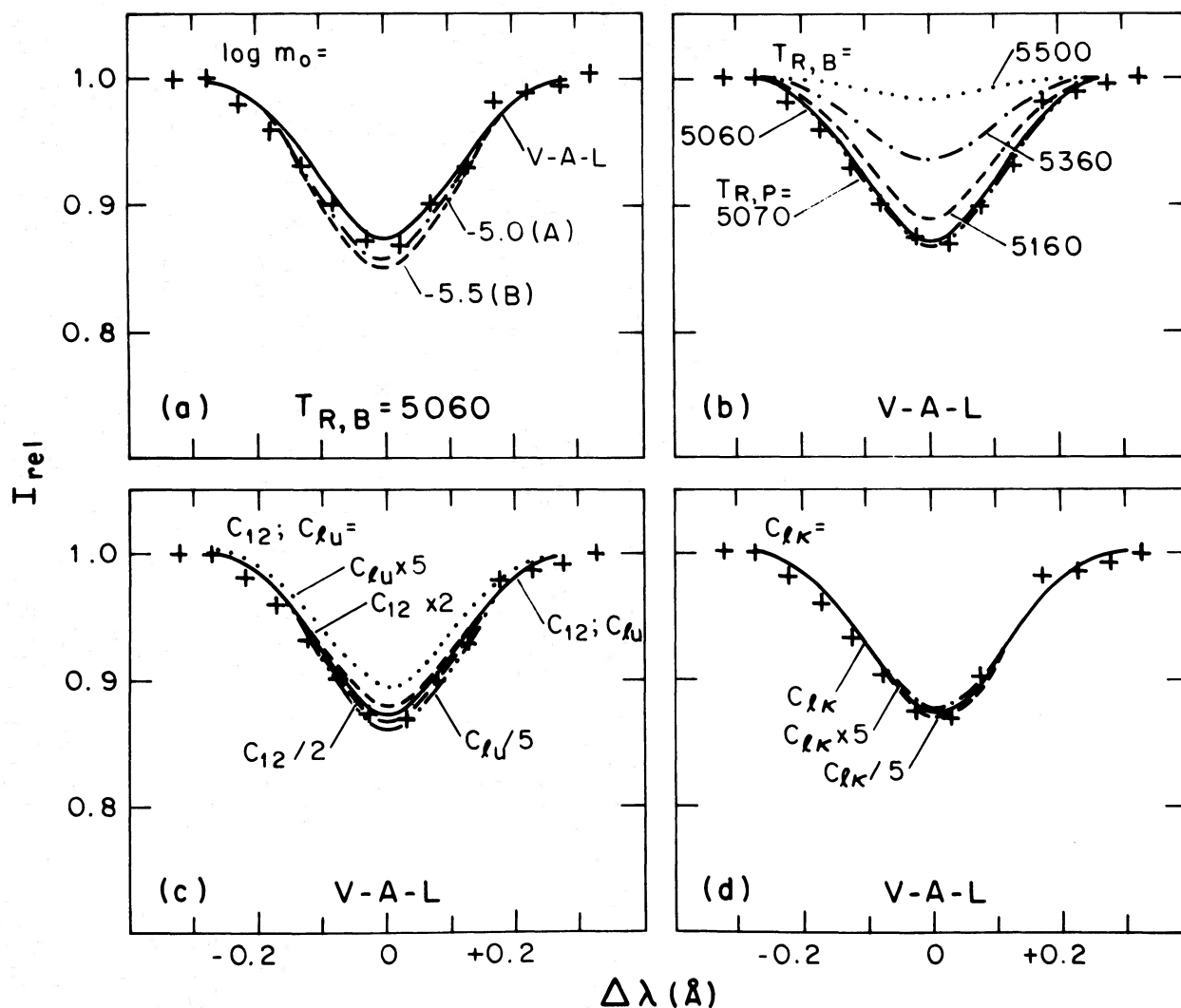


FIG. 6.—Synthesized solar H ϵ profiles showing dependence on model atmospheres, fixed radiative rates, collisional excitation and ionization rates. $T_{R,P}$ is the Paschen continuum radiation temperature.

cross section, and from the resulting rate determined the equivalent value of $T_R^{(0)}$.

Table 1 lists the radiation temperatures we infer from the spectral energy distributions of the Sun and Arcturus illustrated in Figure 5. The probable errors in the inferred radiation temperatures for both stars are on the order of ± 100 K.

V. CALCULATIONS

We use profile synthesis to test the sensitivity of the solar and Arcturus H ϵ features to variations in (1) the model atmospheres; (2) the radiative rates, principally the Balmer and Paschen radiation temperatures $T_{R,B}$ and $T_{R,P}$; and (3) the collisional excitation and ionization rate coefficients. The results are illustrated in Figures 6a–6d for the Sun and Figures 7a–7d for Arcturus. Notice that factor-of-5 enhancements of the

$l \geq 2$ collisional excitation and ionization rate coefficients above their nominal values have little effect on the emergent profiles of H ϵ for both stars. This is fortunate because the estimated coefficients may be only order-of-magnitude accurate. The apparent insensitivity of H ϵ to the collisional rates coupled with the significant dependence of the profiles on the Balmer radiation temperature (note: $\Delta T_{R,B} = 100$ K corresponds to a roughly 20% increase in the $l = 2$ photoionization rate) is consistent with the notion that the Balmer series is photoionization-dominated in both stars (e.g., Thomas and Athay 1961; Ayres and Linsky 1974; Fosbury 1974). Perhaps fortuitously, the synthesized H ϵ absorption profiles for the solar models show good agreement with the observed profile for the empirically derived Balmer radiation temperature $T_{R,B} = 5060 \pm 100$ K. Most significant, though, is the marked dependence of the Arcturus H ϵ emission on

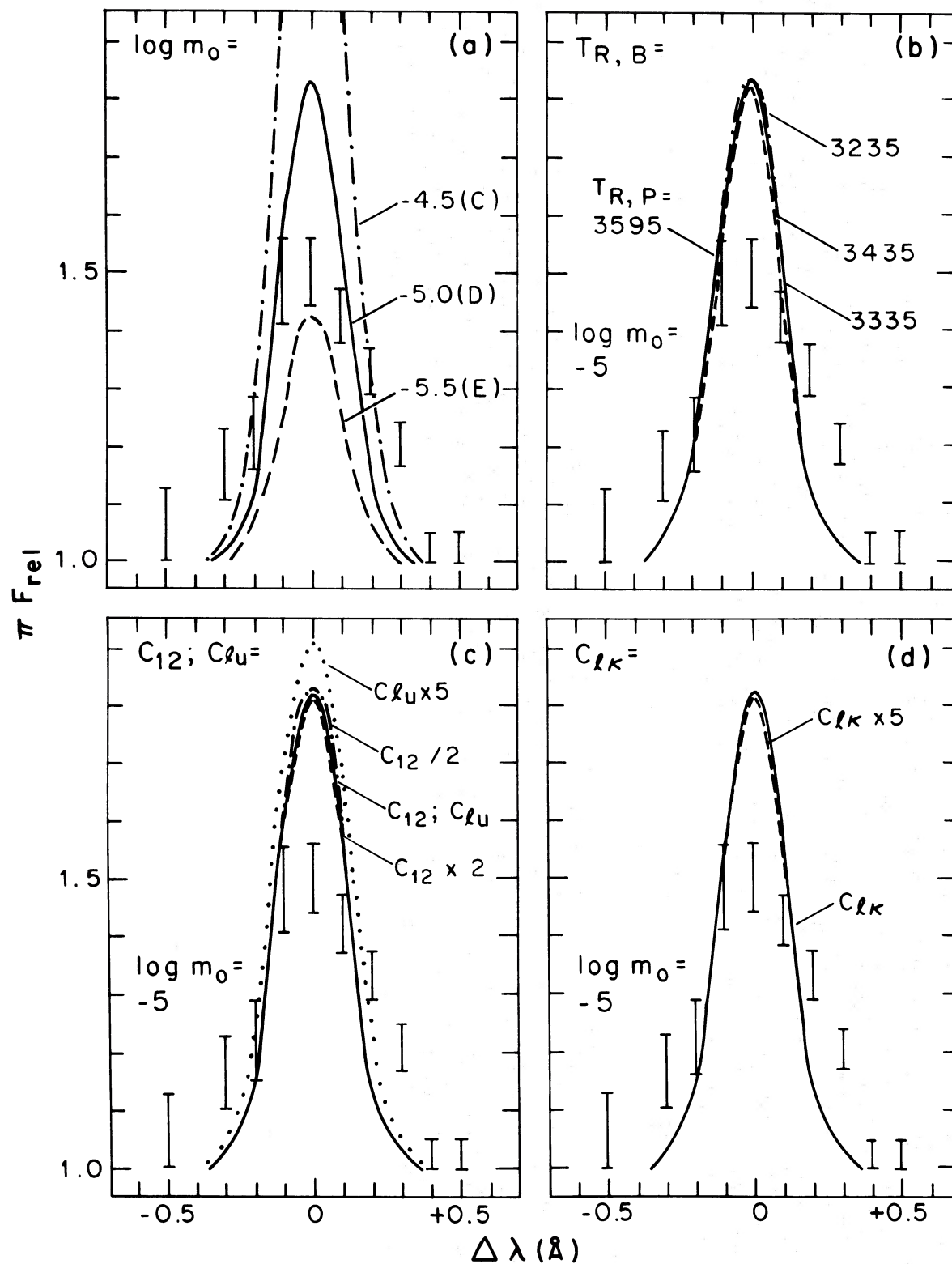


FIG. 7.—Same as Fig. 6, but for Arcturus

the chromosphere model, in contrast to the solar feature which shows little sensitivity to either the model chromosphere or photosphere.

The fact that the Arcturus $H\epsilon$ emission is sensitive to the chromospheric temperature rise but the solar feature is not may seem somewhat surprising, but the explanation is simple: Arcturus has a much smaller photospheric contribution to the total n_2 column density than the Sun because only in Arcturus's chromosphere are the kinetic temperatures high enough to significantly populate the second level without completely ionizing hydrogen. In the Sun, on the other hand, the chromospheric contribution to $\tau_{H\epsilon}$ is small compared with that provided by the "hot" photosphere with its comparable temperatures but much higher densities.

This curious dichotomy is illustrated in Figures 3 and 4 which, in addition to the model atmospheres, depict opacity contribution functions for the V-A-L solar model (Fig. 3) and the Arcturus model D (Fig. 4). The quantity plotted is

$$\tilde{c}_2(m) = \frac{n_2(m)}{n_H(m)} \frac{m}{\log e}. \quad (20)$$

It can easily be shown that for any of the Balmer lines, in particular $H\epsilon$, the frequency-integrated optical depth is proportional to

$$\tau_{2j}(m') \propto \int_{-\infty}^{\log m'} \tilde{c}_2(m) d \log m. \quad (21)$$

From the two \tilde{c}_2 curves it is clear that the $H\epsilon$ opacity contribution for $\tau_{H \text{ wing}} \lesssim 1$ is dominated by the photosphere in the Sun but by the chromosphere in Arcturus. This result suggests that because the n_2 population is very temperature sensitive, relatively small changes in Arcturus's chromospheric temperature structure should have a substantial effect on the total $H\epsilon$ optical depth for $\tau_{H \text{ wing}} \lesssim 1$, and hence should affect the $H\epsilon$ emission contrast. In fact, since the chromospheric $H\epsilon$ line-center optical depth is itself small (~ 0.3 for model D), the essentially optically thin $H\epsilon$ "emission" (note: $S_{H\epsilon} \gg S_{H \text{ wing}}$ at and above $\tau_{H \text{ wing}} \sim 1$) should be very sensitive to the chromospheric model. On the other hand, since the chromospheric contribution to the total solar $H\epsilon$ optical depth for $\tau_{H \text{ wing}} \lesssim 1$ is small compared with the photospheric contribution, the solar $H\epsilon$ feature should be relatively insensitive to changes in the chromospheric model.

VI. DISCUSSION

Wilson (1957) finds a weak correlation of the $H\epsilon$ and Ca II emission intensities, especially among K and M giants. This result is easy to understand if the $H\epsilon$ emission contrast (the quantity measured by Wilson) is sensitive to the chromospheric temperature rise in cool giants in general, as we have found for Arcturus in particular, because the Ca II resonance line emission itself is known to vary substantially with changes in the chromospheric temperature gradient

owing to the collision dominated H and K source functions (e.g., Athay and Skumanich 1968; Linsky and Avrett 1970; Paper III). Furthermore, $H\epsilon$ emission is likely to favor low-gravity stars, because the H wing is broader than in main-sequence stars (Lutz *et al.* 1973); hence the radiation field background at $H\epsilon$ is depressed. The large scatter Wilson finds away from a strict $H\epsilon$ -Ca II emission strength correlation could be attributed to (1) gravity- and abundance-dependent variations in the H wing background, which affect the $H\epsilon$ emission contrast; (2) null correlations for "hot" stars with "thin" chromospheres where $H\epsilon$ is primarily a *photospheric* feature; and (3) observational errors (see Wilson 1957). Although the latter factor may be substantial, because the $H\epsilon$ intensities were eye-estimated from plates exposed for the Ca II lines rather than $H\epsilon$, we suspect that the other two factors may play an important role. In addition, Fosbury (1974) points out that for a certain class of cool dwarfs, in particular the dMe stars, the Balmer lines might become collision dominated owing to the much reduced background radiation fields. In such stars $H\epsilon$ emission might also show sensitivity to the chromospheric temperature rise, but for a different reason than the apparent sensitivity shown by the Arcturus feature: in the dMe stars the chromosphere would directly affect the $H\epsilon$ source function through collisional coupling to the temperature rise, while in Arcturus the chromosphere affects primarily the absolute n_2 column density. We reiterate that the $H\epsilon$ source functions for both the Sun and Arcturus are dominated by the Balmer radiation field.

The significant result of our differential analysis of the solar and Arcturan $H\epsilon$ features is that the emission contrast in the cool giant is sensitive to the chromospheric temperature rise. In fact, because the $H\epsilon$ emission depends on the details of the model chromosphere in a different way from the more familiar Ca II H and K and Mg II *h* and *k* lines, $H\epsilon$ profile synthesis could provide a consistency check for models of cool giants inferred from observations of the Ca II and Mg II emission. Interestingly, the Arcturus chromosphere models which show good agreement with the observed $H\epsilon$ emission are also reasonably consistent with the range of models inferred from the H, K, and *k* lines in Paper III. While this result may be fortuitous, it does suggest that our approach of considering only a simple class of chromosphere models may be adequate, especially considering the large uncertainties inherent in the stellar observations.

We would hope, therefore, that further observations of the stellar $H\epsilon$ feature could be undertaken, especially of $H\epsilon$ emission in cool giants with simultaneous measurements of the Ca II intensities. Such observations would require high spectral dispersion, low scattered light, and the possibility of accurately calibrating the $H\epsilon$ profile in absolute flux units, so that the important effect of the gravity-dependent variations in the H wing background from star to star could be taken into account. Observations of this nature would be of great use in the continuing systematic study of chromospheric structure in late-type stars.

We gratefully acknowledge the support of the National Center for Atmospheric Research, operated by the University Corporation for Atmospheric Research under contract with the National Science Foundation, which provided computing time. We

thank J. N. Heasley and R. A. Shine for their helpful advice. This work was supported in part through grants NAS 5-23274 and NGR-06-003-057 from the National Aeronautics and Space Administration to the University of Colorado.

REFERENCES

- Athay, R. G., and Skumanich, A. 1968, *Solar Phys.*, **3**, 181.
 Auer, L. H., Heasley, J. N., and Milkey, R. W. 1972, *KPNO Contr.*, No. 555.
 Auer, L. H., and Mihalas, D. 1969, *Ap. J.*, **158**, 641.
 Ayres, T. R., and Linsky, J. L. 1974, *Bull. AAS*, **6**, 226.
 ———. 1975, *Ap. J.*, in press (Paper III).
 Ayres, T. R., Linsky, J. L., and Shine, R. A. 1975, *Bull. AAS* (in press).
 Canfield, R. C. 1971a, *Astr. and Ap.*, **10**, 54.
 ———. 1971b, *ibid.*, p. 64.
 Carbon, D. F., and Gingerich, O. 1969, *Proceedings of the Third Harvard Smithsonian Conference on Stellar Atmospheres*, ed. O. Gingerich (Cambridge, Mass.: MIT Press), p. 377.
 Crandall, D. H., Dunn, G. H., Gallagher, A., Hummer, D. G., Kunasz, C. V., Leep, D., and Taylor, P. O. 1974, *Ap. J.*, **191**, 789.
 Doherty, L. R. 1972, *Ap. J.*, **178**, 495.
 Dupree, A. K. 1972, *Ap. J.*, **178**, 527.
 Fosbury, R. A. E. 1971, *M.N.R.A.S.*, **155**, 7P.
 ———. 1974, *ibid.*, **169**, 147.
 Gingerich, O., Noyes, R. W., Kalkofen, W., and Cuny, Y. 1971, *Solar Phys.*, **18**, 347.
 Golden, L. B., and Sampson, D. H. 1971, *Ap. J.*, **163**, 405.
 Griffin, R. F. 1968, *A Photometric Atlas of the Spectrum of Arcturus* (Cambridge, England: Cambridge Philosophical Society).
 Houtgast, J. 1970, *Solar Phys.*, **15**, 273.
 Kieffer, L. J., and Dunn, G. H. 1966, *Rev. Mod. Phys.*, **38**, 1.
 Linsky, J. L., and Avrett, E. H. 1970, *Pub. A.S.P.*, **82**, 169.
 Lites, B. W. 1974, *Astr. and Ap.*, **30**, 297.
 Lutz, T. E., Furenlid, I., and Lutz, J. H. 1973, *Ap. J.*, **184**, 787.
 Mihalas, D. 1967, *Ap. J.*, **149**, 169.
 ———. 1970, *Stellar Atmospheres* (San Francisco: Freeman).
 Noyes, R. W., and Kalkofen, W. 1970, *Solar Phys.*, **15**, 120.
 Percival, I. C. 1966, *Nucl. Fusion*, **6**, 182.
 Popper, D. M. 1956, *Ap. J.*, **123**, 377.
 Sampson, D. H., and Golden, L. B. 1970, *Ap. J.*, **161**, 321.
 Shine, R. A. 1973, unpublished Ph.D. thesis, University of Colorado.
 Shine, R. A., Milkey, R. W., and Mihalas, D. 1975, *Ap. J.*, **201**, 222.
 Thekaekara, M. P. 1974, *Appl. Opt.*, **13**, 518.
 Thomas, R. N., and Athay, R. G. 1961, *Physics of the Solar Chromosphere* (New York: Interscience).
 Vernazza, J. E., Avrett, E. H., and Loeser, R. 1973, *Ap. J.*, **184**, 605.
 ———. 1975, preprint 215, Center for Astrophysics (V-A-L).
 Wellmann, P. 1940, *Zs. f. Ap.*, **19**, 236.
 Willstrop, R. V. 1965, *Mem. R.A.S.*, **69**, 83.
 ———. 1972, private communication.
 Wilson, O. C. 1938, *Pub. A.S.P.*, **50**, 245.
 ———. 1957, *Ap. J.*, **126**, 46.

THOMAS R. AYRES: Center for Astrophysics, 60 Garden St., Cambridge, MA 02138

JEFFREY L. LINSKY: Joint Institute for Laboratory Astrophysics, University of Colorado, Boulder, CO 80302